

# Effect of interactions on the cellular uptake of nanoparticles

Abhishek Chaudhuri,<sup>1,2,\*</sup> Giuseppe Battaglia,<sup>1</sup> and Ramin Golestanian<sup>2</sup>

<sup>1</sup>*Department of Biomedical Science, University of Sheffield,  
Western Bank, Sheffield S10 2TN, United Kingdom*

<sup>2</sup>*The Rudolf Peierls Centre for Theoretical Physics,  
University of Oxford, 1 Keble Road, Oxford OX1 3NP, United Kingdom*  
(Dated: September 17, 2018)

We present a simple two-state model to understand the size-dependent endocytosis of nanoparticles. Using this model, we elucidate the relevant energy terms required to understand the size-dependent uptake mechanism and verify it by correctly predicting the behavior at large and small particle sizes. In the absence of interactions between the nanoparticles we observe an asymmetric distribution of sizes with maximum uptake at intermediate sizes and a minimum size cut-off below which there can be no endocytosis. Including the effect of interactions in our model has remarkable effects on the uptake characteristics. Attractive interactions shift the minimum size cut-off and increase the optimal uptake while repulsive interactions make the distribution more symmetric lowering the optimal uptake.

## INTRODUCTION

The endocytic process [1, 2] is of paramount importance to understanding the cellular uptake of nano-materials, essential for the development of gene and targeted drug delivery tools. A key feature in the development of such tools is to achieve effective cytosolic delivery. To this purpose there have been experiments using liposomes [3], nanoparticles (NPs) [4], polymerosomes [5–7], nanotubes [8, 9], electroporation [10] and ultrasonic treatments [11]. Several of these techniques also suffer from the problem of high levels of cytotoxicity although recent experiments using polymerosomes overcome this shortcoming.

In several of these experiments using gold and silver nanoparticles, nanotubes and polymerosomes [5–7, 9, 12–17] particle size plays an important role in the cellular uptake. These experiments suggest that endocytosis of NPs is receptor-mediated and that there is an optimal size where the uptake is maximum. Most theoretical approaches [18–21] to study the effect of NP geometry on cellular uptake predict a threshold radius below which there can be no cellular uptake, and an asymmetric distribution of the uptake which decays with particle size. Although these approaches correctly predict the size where the uptake is optimal ( $\sim 20 - 30$  nm), experimentally the distribution is symmetric and does not seem to agree with the lower bound as predicted from the theories [15, 16]. The answer to this anomaly could be hidden in the highly complex endocytic mechanism itself.

The endocytic process involves the selection and segregation of the cargo at the cell surface, subsequent invagination and pinching off from the cell membrane, and, finally, the transport of these vesicles to intracellular compartments where they fuse with the target membrane. The mechanisms by which specific cargo are internalized differ in their morphological and biochemical details [1, 2, 22]. However, recent evidence [23] suggests the need to consider the sharing of molecular machinery de-

pending on the nature of the cargo and to understand the basic physical principles common to these different uptake mechanisms.

A key step in the endocytic process is the segregation and clustering of cargo on the cell membrane which are believed to be the sites where molecular machinery may be recruited to generate membrane curvature, form membrane invaginations and subsequently cause scission [1, 23]. The mechanisms of formation of these nanodomains can be both passive and active. Although passive clustering which does not involve ATP hydrolysis can occur via intermolecular cargo interactions, Reynwar et. al. [24] showed using coarse grained simulations, that curvature-inducing model proteins adsorbed on lipid bilayer membranes could experience attractive interactions that occur purely as a result of membrane curvature. These interactions could result in clustering and subsequent invaginations. Thus passive clustering can happen even in the absence of specific cargo interactions. An example of the passive clustering is the binding of Shiga toxin—a bacterial toxin—to glycolipid receptors, Gb3, in the cell membrane of certain cell types [25, 26]. Although the Shiga toxin molecules do not interact directly, they induce the clustering of the Gb3 lipids, thereby causing local membrane curvature.

The active mechanisms for cell surface clustering requires ATP and are therefore energy dependent processes. An example of active clustering is the formation of nanoscale clusters of glycosylphosphatidylinositol anchored proteins (GPI-AP) on the cell membrane which are required for their subsequent endocytosis [27]. These proteins exist as monomers and nanoclusters ( $\sim 4 - 6$  nm in size, consisting of  $< 5$  molecules) with the interconversion between the two being spatially heterogeneous, being coupled to an active cortical cytoskeleton. Perturbing the cortical actin activity affects the construction, dynamics and spatial organization of these nanoclusters [28]. This type of active segregation also happens with gan-

glisides GM1 and GM3 in the exoplasmic (outer) leaflet [29] and Ras isoforms in the cytoplasmic (inner) leaflet of the plasma membrane [30].

The above examples of passive and active clustering do not involve the clathrin mediated endocytic pathway where the entrapment of the cargo occurs by its association with adapter proteins. However, even in the clathrin coat mediated endocytic pathway, the clathrin lattice organizes the epsins or BAR domain proteins into domains, which then locally deform the membrane [31, 32]. Therefore the segregation and clustering of cargo on the cell surface is highly important in the endocytic process. This naturally raises the following questions: could cell surface clustering affect the size-dependent cellular uptake of NPs and if so how could we model the clustering process? Recent experiments [9] have shown evidence of NP surface clustering on the cell membrane and it is important to investigate this in some detail.

Here, we study systematically for the first time, the effect of interactions on the cellular uptake of NPs using a thermodynamic model first proposed by Tzlil et al. [18, 33] and subsequently studied by Zhang et al. [19] in the NP context. We develop our model by incorporating interactions between NPs. Using a simplified two-state version of the model, we then elucidate the relevant energy terms which affect the uptake of NPs in the absence of interactions. We then show that interactions between NPs indeed affect the minimum radius of uptake as well as the distribution.

## THE MODEL

In this model, the system, which consists of a cell and ligand-coated spherical NPs in a solution, is in a thermodynamic equilibrium at which a certain number of NPs are endocytosed. At this state,  $N$  NPs adhere to the cell surface that contains  $L$  receptors via ligand-receptor binding, and are wrapped to different extents by the cell membrane (see Fig. 1). The receptors diffuse freely on the cell surface and are segregated into  $L_p$  free receptors in the planar membrane and  $L_b$  bound receptors in the curved regions. Let  $A$  be the cross-sectional area of a receptor. For a given NP radius  $R$ , the number of receptors that can attach to the NP is  $K = 4\pi R^2/A$ . For convenience, we shall choose  $A$  as our unit of area and  $\sqrt{A} = R\sqrt{4\pi/K}$  as our unit of length. The total membrane area is denoted by  $MA$  (in units of  $A$ ) and is therefore the total number of sites on the membrane that are accessible to the receptors. The surface concentration of NPs is then  $c = N/MA$ .

We have assumed that the time scale for endocytosis is much larger than the time for the receptors to diffuse and segregate into the curved and planar regions. Therefore the distribution of wrapping sizes and receptor densities can be treated using equilibrium statistical mechanics.

Let  $n_k$  denote the number of NPs wrapped by a membrane section of area  $k$  where  $k$  varies discretely between  $k = 0$  (unwrapped state) and  $k = K$  (completely wrapped state). Then, we have

$$N = \sum_{k=0}^K n_k, \quad (1)$$

and

$$M_b = \sum_{k=0}^K k n_k, \quad (2)$$

where  $M_b A$  is the total curved membrane area associated with the wrapped NPs and  $M_p A = (M - M_b)A$  is the total area of the planar regions. The binding of a ligand and a receptor releases chemical energy,  $\epsilon$ , which drives the wrapping at the cost of the energy required to bend the membrane. Therefore, the diffusion of receptors inside the curved regions should lower the energy of the system facilitating wrapping. However, this leads to the segregation of receptors between planar and curved regions, which costs entropy. Also diffusion of free receptors into the curved regions increases the total curved area (more ligand-receptor bonds) and hence increases the total membrane bending energy. Furthermore, attractive (repulsive) interactions between the NPs could lead to clustering (anti-clustering) and therefore affect the wrapping size distribution of NPs. To determine the size distribution of the varyingly wrapped NPs, we first write down the free energy of the system as,

$$\begin{aligned} \frac{\mathcal{F}}{k_B T} &= M_p [\phi_p \ln \phi_p + (1 - \phi_p) \ln(1 - \phi_p)] \\ &+ M_b [\phi_b \ln \phi_b + (1 - \phi_b) \ln(1 - \phi_b)] \\ &+ \sum_k n_k [\ln(n_k/M) - 1] - \epsilon L_b + \hat{\kappa} M_b \\ &+ \sum_k n_k \Lambda_k + \sum_k n_k \Gamma_k + w \sum_{k,k'} k k' n_k n_{k'}, \quad (3) \end{aligned}$$

where  $\phi_p = L_p/M_p A$  and  $\phi_b = L_b/M_b A = (L - L_p)/M_b A$  denote the densities of the receptors in the planar membrane and the wrapped regions respectively,  $k_B$  denoting the Boltzmann constant and  $T$  being the temperature.

The first three terms in the free energy are entropic contributions written in terms of a two dimensional lattice gas model:

- $M_p [\phi_p \ln \phi_p + (1 - \phi_p) \ln(1 - \phi_p)]$  represents the configurational entropy of  $L_p$  free receptors distributed in the  $M_p$  sites of the planar parts of the membrane.
- $M_b [\phi_b \ln \phi_b + (1 - \phi_b) \ln(1 - \phi_b)]$  represents the configurational entropy of distributing  $L_b$  receptors among the  $M_b$  sites of the curved regions.

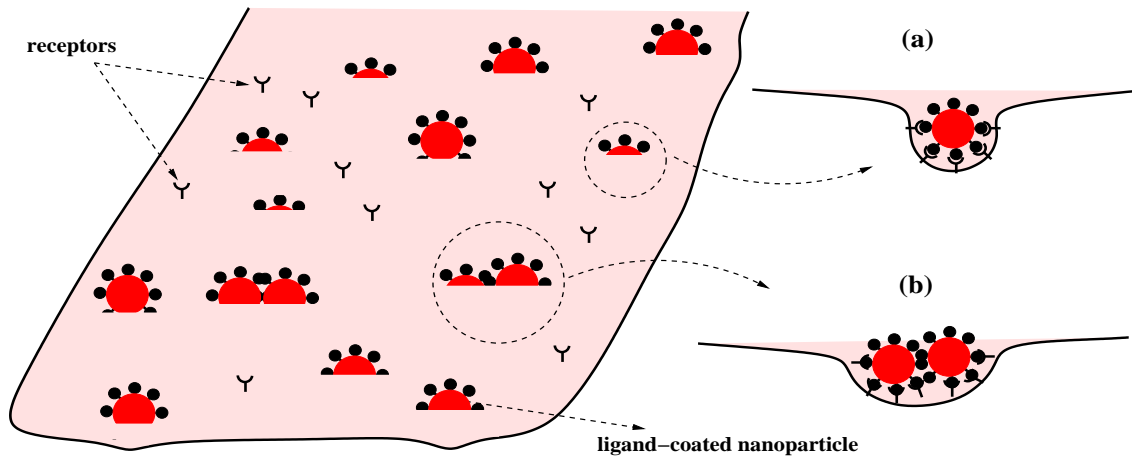


FIG. 1: Schematic figure of adhering NPs wrapped by cell membrane. The NPs are wrapped to different degrees with some of them being internalized. (a) Single NP wrapping showing ligand-receptor binding. (b) Cluster of NPs wrapped by the cell membrane.

- $\sum_k n_k [\ln(n_k/M) - 1]$  is the configurational entropy of a 2D mixture of wrapped NPs when treated as a multicomponent ideal gas. However, we are interested in interacting NPs and would therefore have to include interaction energy for this 2D mixture.

The next five terms are energetic:

- $-\epsilon L_b = -M_b \phi_b \epsilon = -\phi_b \epsilon \sum_k k n_k$  is the total chemical energy released upon the binding of  $L_b$  ligand-receptor pairs.
- $\hat{\kappa} M_b = \hat{\kappa} \sum_k k n_k$  is the total membrane curvature energy in the budding regions. For a spherical geometry, the bending energy per unit area across a NP of radius  $R$  is  $\hat{\kappa} = (\kappa A / 2k_B T)(2/R - c_0)^2$ , where  $\kappa$  denotes the bending modulus. Note that the spontaneous curvature ( $c_0$ ) of cell membranes is nonzero. In our analysis we consider a vanishing spontaneous curvature ( $c_0 = 0$ ). Therefore,  $\hat{\kappa} = 2\kappa A / k_B T R^2 = 8\pi\kappa / k_B T K$ . A positive spontaneous curvature ( $c_0 > 0$ ) could decrease the value of  $\hat{\kappa}$  while a negative spontaneous curvature ( $c_0 < 0$ ) could increase the value of  $\hat{\kappa}$ , for a given value of  $\kappa$ . We shall discuss the effect of spontaneous curvature on cellular uptake later.
- $\sum_k n_k \Gamma_k$ : Total work of pulling excess membrane towards the wrapping sites against lateral tension  $\sigma$ . For a single NP wrapping, the excess area pulled towards the wrapping site is  $4\pi R^2 k^2 / K^2 = k^2 A / K$  [34]. Thus the excess energy is  $\Gamma_k = \sigma \times \text{excess area} = k^2 \sigma A / k_B T K$ .
- $\sum_k n_k \Lambda_k$ : Total line energy of the rim, where  $\Lambda(k)$  denotes the line energy of a  $k$ -bud. Assuming a spherical shape of the membrane at the rim of a

partially wrapped NP,  $\Lambda_k$  is modeled as being proportional to the length,  $\mathcal{L}_k$ , of its rim, with a constant line energy per unit length  $\gamma$  [18]. Therefore,

$$\Lambda_k = \gamma \mathcal{L}_k = \gamma 2\pi R \sqrt{4 \frac{k}{K} \left(1 - \frac{k}{K}\right)}. \quad (4)$$

Note that  $\mathcal{L}_k$  vanishes for  $k = 0$  and  $k = K$  and is maximum ( $2\pi R$ ) for a half-wrapped NP ( $k = K/2$ ). However, the local wrapping behavior of the membrane to a NP is different from the assumption made above [34, 35]. We need to consider an additional bending energy for the unadsorbed membrane detaching from the NP at the rim. Although the  $k$ -dependence of this energy is different from the simple form assumed in Eq. (4), the general features of large energies for half-wrapped state ( $k = K/2$ ) and very small energies for unwrapped and completely wrapped states are the same.

- $w \sum_{k,k'} k k' n_k n_{k'} = w \left[ \sum_k k n_k \right] \left[ \sum_{k'} k' n_{k'} \right] = w M_b^2$  is the interaction energy between the partially wrapped NPs,  $w$  denoting the strength of the interaction (or the second virial coefficient). We assume the interaction to depend on the degree of deformation and curvature of nearby curved membrane patches and therefore to the degree of wrapping of the cell membrane to individual NPs. Thus the total interaction energy when summed over is proportional to the total curved area. Interaction between membrane inclusions or adsorbates could arise due to a variety of different mechanisms [36] including membrane fluctuations [37, 38].

In the final stages of endocytosis the membrane wrapped NP pinches off which results in a topology change. This

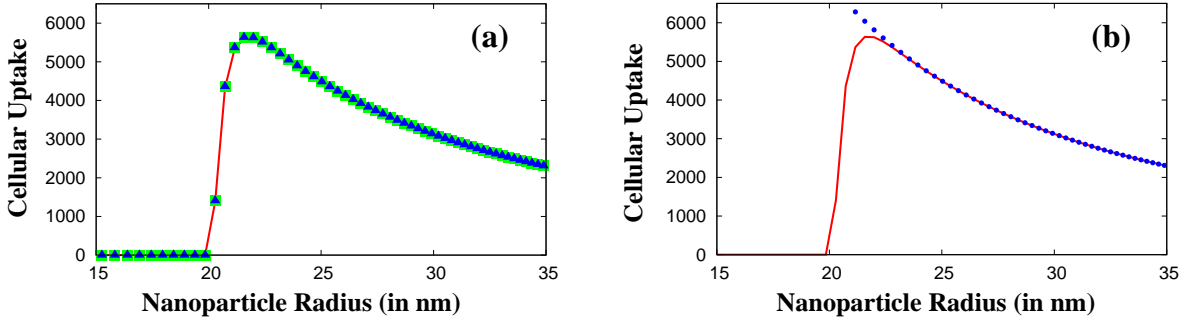


FIG. 2: Size dependent cellular uptake of non-interacting NPs. (a) The red line is for the two-state model with  $\Lambda_k = 0 = \Gamma_k$ , the green ( $\square$ ) and blue ( $\triangle$ ) points are for the  $K$ -state system with  $\Gamma_k = 0$  and  $\Gamma_k \neq 0$  respectively. (b) The red line is for the two-state model while the blue ( $\bullet$ ) points indicate the large  $R$  behaviour.

severing mechanism of the wrapped NP from the membrane is brought about by proteins such as dynamin and C-terminal binding protein 3/brefeldin A-ribosylated substrate (CtBP3/BARS). According to Gauss-Bonnet theorem [39], this leads to an increase of  $4\pi\bar{\kappa}$  in Gaussian bending energy, with  $\bar{\kappa}$  representing the Gaussian bending rigidity of the cell membrane. In our model we are interested in events prior to the final scission process and will therefore safely ignore this term. In fact, all partially wrapped NPs for which  $k \geq 0.9K$  will be assumed to be endocytosed.

To find the equilibrium state of the system we minimize the free energy with respect to  $L_b$  and  $n_k$ . From  $\partial\mathcal{F}/\partial L_b = 0$ , we have

$$\frac{\phi_p}{1 - \phi_p} = \frac{\phi_b}{1 - \phi_b} e^{-\epsilon}. \quad (5)$$

Minimizing  $\mathcal{F}$  subject to the constraint of Eq. (1), we get the normalized wrapping size distribution as

$$p_k = \frac{n_k}{N} = \frac{e^{-\beta_k} \alpha^k}{\sum_{k=0}^K e^{-\beta_k} \alpha^k}, \quad (6)$$

where we have defined

$$\alpha = (\phi_p/\phi_b) e^{\epsilon - \hat{\kappa}}, \quad (7)$$

and

$$\begin{aligned} \beta_k &= \Lambda_k + \Gamma_k + 2wk \sum_{k'} k' n_{k'} \\ &= \Lambda_k + \Gamma_k + 2wcMk \sum_{k'} k' p_{k'}. \end{aligned} \quad (8)$$

The conservation condition for the receptors gives

$$\phi_p (1 - c \sum_k k p_k) + \phi_b c \sum_k k p_k = \phi_0. \quad (9)$$

The densities of the receptors  $\phi_p$  and  $\phi_b$  can be obtained by numerically solving Equations (5)-(9). Substituting

$\phi_p$  and  $\phi_b$  back into Eq. (6) yields the wrapping size distribution, and hence the number of fully internalized NPs

$$n_K = cM p_K. \quad (10)$$

Therefore,  $n_K$  gives the cellular uptake of nanoparticles. We first study the effect of particle size on the cellular uptake of non-interacting NPs and then see the effect of interactions on the distribution.

The choice of the physical constants is mostly guided by experimental data although there are some free parameters as well. The bending modulus ( $\kappa$ ) of biomembranes is typically on the order of  $20 k_B T$  [40, 41]. The receptor-ligand binding energy,  $\epsilon$  is assumed to be comparable to antibody-antigen interaction and is estimated to be on the order of  $15 - 25 k_B T$  [42, 43]. The length scale is set by the length of the receptor ( $\sqrt{A}$ ) which is typically on the order of  $15 \text{ nm}$ . Therefore,  $A \sim 225 \text{ nm}^2$ . Experimental information suggests that the number of receptors varies from  $50 - 500 \text{ per } \mu\text{m}^2$  [18, 19, 44, 45]. This implies that  $\phi_0$  could vary from  $0.01$  to  $0.1$ . The concentration of NPs,  $c$ , can vary between  $0.001$  and  $0.005$ . The diameter of the cell being  $\approx 15 \mu\text{m}$ , the surface area of the cell is  $\approx 707 \mu\text{m}^2$ . Therefore,  $M = 3.14 \times 10^6$ . In our numerical analysis, we choose  $\kappa = 20 k_B T$ ,  $\epsilon = 25 k_B T$ ,  $c = 0.003$ ,  $\phi_0 = 0.05$ , and  $M = 3.14 \times 10^6$  [18, 19]. In what follows, we choose  $\sigma = 0$  and consider the effect of  $\sigma$  on uptake in a later section. Both  $\gamma$  and  $w$  are free variables and we choose  $\gamma = 1.0$  (in units of  $k_B T$  per unit length,  $\sqrt{A}$ ).  $w$  is varied from zero (non-interacting) to positive (repulsion) and negative (attraction) values.

## TWO-STATE MODEL

To analyze the size-dependent uptake of NPs we make a major simplification in the model. We assume that the

NPs upon arrival to the cell surface are either endocytosed completely or remain free without there being any intermediate wrapped state. Then the model essentially reduces to a two-state model with the two states being  $k = 0$  and  $k = K$ . Our goal is to come up with the minimal model to understand the experimental uptake behavior and to find the only relevant energetic contributions. Note that the line energy term ( $\Lambda_k$ ) automatically vanishes with this simplifying assumption. We now study the uptake behavior (i) in the absence of interactions and (ii) when the NPs interact.

**(i) Non-interacting case ( $w = 0$ )**

With the two-state model, in the absence of interactions and with  $\Lambda_k = 0 = \Gamma_k$ , we observe [Fig. 2(a)] that below a critical radius,  $R_{\min}$ , there is hardly any uptake. Above  $R_{\min}$ , the uptake increases sharply to reach a maximum and then decays as a power law with increasing radius. Thus, the two-state model correctly reproduces the optimal uptake behavior at intermediate radii seen in experiments. We compare our results for the two-state model with the full K-state model both in the presence and absence of the  $\Gamma_k$  term. We find that for  $\gamma = 1$  and  $\sigma = 0.001$  (in units of  $k_B T$  per unit area) the surface tension term does not affect the size-dependent distribution significantly. As we shall show later, increasing  $\sigma$  decreases uptake significantly although the uptake characteristics remain unchanged. Thus we conclude that the only relevant energy terms in understanding the size-dependent endocytosis of NPs are the energy released on ligand-receptor binding and the energy cost in bending the membrane. We verify this further by analyzing the behavior at large and small radii.

**Behavior at large  $R$ .** For the two state model, Eq. (9) (the conservation condition) reduces to giving the completely wrapped particle size distribution as

$$p_K = \left[ \frac{\phi_0 - \phi_p}{\phi_b - \phi_p} \right] \frac{1}{cK} \quad (11)$$

In the large  $R$  limit (or large  $K$  limit), the receptor density in the fully enveloped NPs is almost saturated,  $\phi_b \approx 1$ , whereas the free receptor density is negligible  $\phi_p \approx 0$ . Then

$$p_K \approx \frac{\phi_0}{cK} = \frac{\phi_0 A}{4\pi c R^2}. \quad (12)$$

Therefore, cellular uptake for larger NPs is inversely proportional to the square of the size of the NPs and reproduces the numerically predicted behavior at large radius exactly [Fig. 2(b)].

**Behavior at small  $R$ .** To understand the low cellular uptake at smaller radii we follow Tzllil et al. to make

the *macroscopic (bud) phase approximation*, i.e. assume that instead of the curved regions being made up of several NPs wrapped to different extents, there is a single NP with wrapped area  $M_b$  that coexists with the planar membrane phase. This approximation causes the configurational entropy of the NPs in the free energy expression to drop off. Also  $\Lambda_k = 0$  for all  $k$ . Minimizing the resulting free energy with respect to  $L_b$  gives Eq. (5) and minimizing it with respect to  $M_b$  yields

$$\frac{1}{1 - \phi_p} = \frac{1}{1 - \phi_b} e^{-\hat{\kappa}}. \quad (13)$$

Solving Eqs. (5) and (13) we can determine the receptor densities in the two coexisting phases as [18]

$$\phi_b = \frac{1 - e^{-\hat{\kappa}}}{1 - e^{-\epsilon}} \quad \text{and} \quad \phi_p = \frac{e^{\hat{\kappa}} - 1}{e^{\epsilon} - 1}. \quad (14)$$

Therefore, we can have coexistence between the planar and wrapped phases only if  $\epsilon \geq \hat{\kappa} \geq 0$ . Thus, for a single wrapped NP,  $\epsilon = \hat{\kappa}$  is the critical value below which we cannot have wrapping. Substituting for  $\hat{\kappa}$ , we get the critical radius for the onset of wrapping as [46],

$$R_{\min} = \sqrt{2\kappa A/\epsilon} \quad (15)$$

For the values of  $\kappa$  and  $\epsilon$  used in the numerical estimates we get  $R_{\min} \approx 19$  nm.

**(ii) Interacting case ( $w \neq 0$ )**

As observed above, the uptake of NPs in the absence of interactions is highly asymmetric and also predicts a lower radius cut-off. Experimentally, the distribution has found to be rather symmetric both for Au nanoparticles [15, 16] and DNA wrapped single-walled carbon nanotubes (DNA-SWNT) [9]. Moreover, there is significant internalization of particles below the minimum radius predicted by the model. Experiments using DNA-SWNT show an increase in near-infrared fluorescence from SWNT concentrated at the external cell membrane during the early stages of endocytosis mechanism [9], indicating possible clustering of nanotubes on the cell surface prior to uptake. To incorporate clustering in our model, we include an effective interaction in our model. The idea is that interactions could lead to clustering which could drive wrapping of NPs of smaller sizes. In our model, the interaction between NPs is controlled by the interaction parameter,  $w$ . Negative  $w$  implies attraction while positive  $w$  implies repulsion. We do our analysis for the two-state model.

**Results for attraction ( $w < 0$ ).** Figure 3(a) shows the results for size-dependent uptake of NPs in the presence of attractive interaction. Similar to the behavior in the absence of interactions, we find that below  $R_{\min}$ , there is hardly any endocytosis. Above  $R_{\min}$ , the uptake

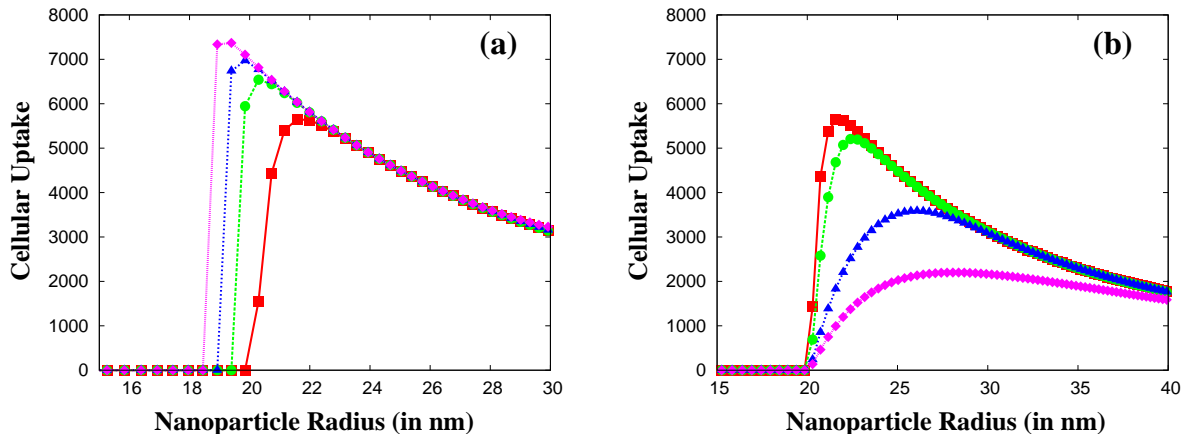


FIG. 3: Size dependent cellular uptake of interacting NPs. (a) The curves are for different values of  $w = 0.0$  (red,  $\square$ ),  $w = -0.00002$  (green,  $\circ$ ),  $w = -0.00003$  (blue,  $\triangle$ ), and  $w = -0.00004$  (pink,  $\diamond$ ).  $R_{\min}$  decreases with increasing strength while the optimal uptake increases. (b) The curves are for different values of  $w = 0.0$  (red,  $\square$ ),  $w = 0.00001$  (green,  $\circ$ ),  $w = 0.00005$  (blue,  $\triangle$ ), and  $w = 0.0001$  (pink,  $\diamond$ ). Optimal uptake decreases with increasing repulsion.

increases rapidly, and subsequently reaches a maximum and then decays slowly. We note, however, that the uptake mechanism is strongly dependent on the value of  $w$ . With the increase in the strength of the attractive interaction, (increasing  $|w|$ ), the minimum radius for uptake,  $R_{\min}$ , decreases substantially. Also the maximum uptake increases with increasing  $|w|$  indicating that uptake becomes more favorable in such circumstances. To explain this behavior we need to look carefully at the energetics. Without interactions, the low radius cut-off is determined by the competition between the energy released on ligand-receptor binding and the energy cost in bending the membrane. Attractive interactions cluster NPs and lower the free energy locally so that the system can afford to pay the cost of membrane bending energy, resulting in endocytosis for smaller particle sizes that would otherwise have been prohibited.

**Results for repulsion ( $w > 0$ ).** Figure 3(b) shows the results for size-dependent uptake of NPs in the presence of repulsive interaction. We find that the behavior is distinctly different from that with attractive interactions. Although the uptake mechanism strongly depends on the interaction strength  $w$ , the characteristics differ significantly. Interestingly, the lower radius cut-off  $R_{\min}$  does not shift with increasing  $w$  and is the same for all  $w$  values. The maximum uptake however decreases with increasing  $w$ . The uptake behavior at large  $R$  is also affected. Although the uptake decreases at large  $R$ , the decay is much slower as  $w$  increases. This behavior can again be explained by looking at the energetics. Repulsion between NPs (positive  $w$ ), pushes them apart and the energetics at lower radius are governed by the same single NP wrapping energetics as in the absence of interactions. Therefore,  $R_{\min}$  does not change when we in-

crease  $w$ . However, the uptake for  $R > R_{\min}$  is affected since positive  $w$  increases the *global* free energy cost, thus decreasing the optimal uptake and affecting the behavior at large radius making the uptake more symmetric with particle size.

Therefore, we find that interactions affect cellular uptake of NPs significantly. We studied the two cases of attractive and repulsive interactions separately. However, in the physical system, we expect both of these interactions to be present simultaneously with attractive interaction affecting the uptake of smaller particles and repulsion dominating for the bigger ones. Such a picture could provide a qualitative understanding of the experimental observation of size-dependent cellular uptake of NPs.

#### Effect of membrane tension and spontaneous curvature

The effect of membrane tension is to lower the optimal uptake of NPs [47, 48]. In Fig. 4 we show the variation of uptake with system size for different values of the surface tension  $\sigma$  (in units of  $k_B T$  per unit area) in the absence of interactions. The nature of cellular uptake with the particle size remains the same for different values of  $\sigma$  although the amount of uptake decreases.

In all our analysis we have ignored the effect of spontaneous curvature ( $c_0$ ). As we have mentioned earlier, a non-zero  $c_0$  could lower or raise the value of  $\hat{\kappa}$  which should in turn lower or raise the free energy barrier for the uptake of a nanoparticle. Hence the optimal uptake could indeed be lower or higher depending on the value of  $c_0$ . However, the characteristics of uptake behavior is not altered.

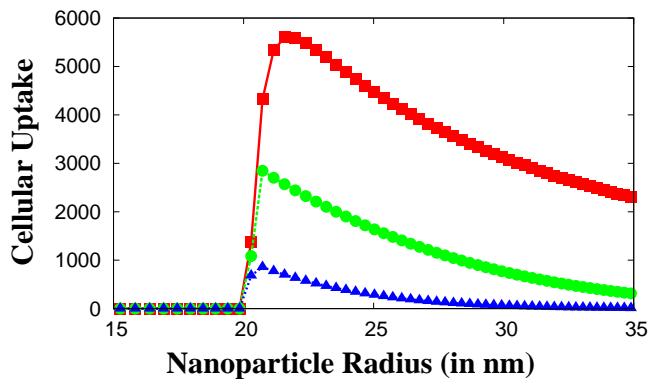


FIG. 4: Size dependent cellular uptake of non-interacting NPs for different values of  $\sigma = 0.001$  (red,  $\square$ ),  $\sigma = 0.02$  (green,  $\circ$ ) and  $\sigma = 0.1$  (blue,  $\triangle$ ).

## SUMMARY AND CONCLUSION

In this paper, we have studied the effect of interactions between surface-bound NPs on their subsequent endocytosis in the context of a statistical thermodynamic model. One of our first results is to clearly show the relevant energy terms required to understand the uptake mechanism qualitatively. To do so, we simplified our model to a two-state model, which captures the essential features of the uptake behavior. We showed that apart from the important entropic contributions coming from the distribution of the receptors and the NPs on the cell surface, the energy terms that dictate the uptake characteristics are the energy released via ligand-receptor binding and the energy cost in bending the membrane. Although we show that the line energy and energy in pulling excess membrane area are not significant when the aim is to understand the specific uptake behavior, we do not rule out the importance of these terms in the endocytic process. These energy terms, as well as the Gaussian bending energy during the pinch-off, are relevant for the studies of membrane invaginations and wrapping. However, they may be dispensable when addressing the question of the number of NPs endocytosed at a given time.

Beyond the two-state model, our results show that interactions between NPs could have a drastic effect on the uptake process. Attractive interactions lead to clustering of NPs, which effectively lowers the free energy threshold for wrapping and therefore shifts the lower cut-off radius. This is not possible in the absence of interactions unless, of course, we changed the relative values of  $\kappa$  and  $\epsilon$ . For fixed  $\kappa$  and  $\epsilon$ , we see that repulsive interactions also have a significant impact, in that they cause the cellular uptake to be reduced and modify uptake characteristics towards being more symmetric.

In our model, interactions are assumed to be proportional to the wrapped area and the strength of the in-

teraction,  $w$ , is varied freely. Therefore,  $w$  could be thought of as an effective parameter which models the membrane-mediated forces [36]. Müller et al. [49, 50] study the curvature-mediated interaction between particles on the cell surface. From a purely geometric analysis, they showed that the net force between the particles is due to a competition between the force associated with the curvature along the direction joining the particles (which leads to repulsion) and the force associated with the curvatures perpendicular to it (which leads to attraction). It will be interesting to use this kind of model for membrane-mediated interaction in a more detailed study of receptor-mediated endocytosis of interacting NPs.

## ACKNOWLEDGEMENTS

The authors acknowledge fruitful discussions with the members of the ViNCeNS (virus like nanoparticles for targeting the central nervous system) project. This work was supported by grant EP/G062137/1 from the Engineering and Physical Sciences Research Council, United Kingdom.

---

\* Electronic address: a.chaudhuri@physics.ox.ac.uk

- [1] Mayor S and Pagano R 2007 Pathways of clathrin-independent endocytosis *Nat. Rev. Mol. Cell Biol.* **8** 603-612.
- [2] Doherty G J and McMahon H T 2009 Mechanisms of endocytosis *Annu. Rev. Biochem.* **78** 857-902.
- [3] Lasic D D and Papahadjopoulos D 1998 *Medical applications of liposomes* Elsevier, Amsterdam.
- [4] Hu Y, Litwin T, Nagaraja A R, Kwong B, Katz J, et. al 2007 Cytosolic delivery of membrane-impermeable molecules in dendritic cells using pH-responsive core-shell nanoparticles *Nano Lett.* **7** 3056-3064.
- [5] Lomas H, Massignani M, Abdullah A K, LoPresti C, Canton I, et. al. 2008 Non-cytotoxic polymer vesicles for rapid and efficient intracellular delivery *Faraday Discuss.* **139** 143-159.
- [6] Massignani M, LoPresti C, Blanazs A, Madsen J, Armes S P, et. al. 2009 Controlling cellular uptake by surface chemistry, size, and surface topology at the nanoscale *Small* **5** 2424-2432
- [7] LoPresti, C, Lomas H, Massignani M, Smart T and Battaglia G 2009 Polymersomes: nature inspired nanometer sized compartments *J. Mater. Chem.* **19** 3576-3590
- [8] Kostarelou K, Lacerda L, Pastorin G, Wu W, Wieckowski S, et. al. 2006 Cellular uptake of functionalized carbon nanotubes is independent of functional group and cell type *Nat. Nanotech.* **2** 108-113
- [9] Jin H, Heller D A, Sharma R and Strano M S 2009 Size-dependent cellular uptake and expulsion of single-walled carbon nanotubes: single particle tracking and a generic uptake model for nanoparticles *ACS Nano* **3** 149-158

- [10] Neumann E, Schaefer-Ridder M, Wang Y and Hofschneider P H 1982 Gene transfer into mouse lymphoma cells by electroporation in high electric fields. *EMBO J.* **1** 841-845.
- [11] Kim H J, Greenleaf J F, Kinnick R R, Bronk J T and Bolander M E 1996 Ultrasound-Mediated Transfection of Mammalian Cells *Hum. Gene Ther.* **7** 1339-1346.
- [12] Aoyama Y, Kanamori T, Nakai T, Sasaki T, Horiuchi S, et. al. 2003 Artificial viruses and their application to gene delivery. size-controlled gene coating with glycocluster nanoparticles *J. Am. Chem. Soc.* **125** 3455-3457.
- [13] Nakai T, Kanamori T, Sando S and Aoyama Y 2003 Remarkably size-regulated cell invasion by artificial viruses. Saccharide-dependent self-aggregation of glycoviruses and its consequences in glycoviral gene delivery *J. Am. Chem. Soc.* **125** 8465-8475
- [14] Osaki F, Kanamori T, Sando S, Sera T and Aoyama Y 2004 A quantum dot conjugated sugar ball and its cellular uptake. On the size effects of endocytosis in the subviral region *J. Am. Chem. Soc.* **126** 6520-6521
- [15] Chithrani B D, Ghazani A A and Chan W C W 2006 Determining the size and shape dependence of gold nanoparticle uptake into mammalian cells *Nano Lett.* **6** 662-668
- [16] Chithrani B D and Chan W C W 2007 Elucidating the mechanism of cellular uptake and removal of protein-coated gold nanoparticles of different sizes and shapes *Nano Lett.* **7** 1542-1550
- [17] Jiang W, Kim B Y S, Rutka J T and Chan W C W 2008 Nanoparticle-mediated cellular response is size-dependent *Nat. Nanotech.* **3** 145-150
- [18] Tzili S, Deserno M, Gelbart W M and Ben-Shaul A 2004 A Statistical-Thermodynamic Model of Viral Budding *Biophys. J.* **86** 2037-2048
- [19] Zhang S, Li J, Lykotrafitis G, Bao G and Suresh S 2009 Size-dependent endocytosis of nanoparticles *Adv. Mater.* **21** 419-424
- [20] Gao H J, Shi W D and Freund L B 2005 Mechanics of receptor-mediated endocytosis *Proc. Natl. Acad. Sci. USA* **102** 9469-9474
- [21] Bao G and Bao X R 2005 Shedding light on the dynamics of endocytosis and viral budding *Proc. Natl. Acad. Sci. USA* **102** 9997-9998
- [22] Marsh M, and McMahon H T 1999 The structural era of endocytosis *Science* **285** 215-220
- [23] Johannes L and Mayor S 2010 Induced domain formation in endocytic invagination, lipid sorting, and scission *Cell* **142** 507-510
- [24] Reynwar B J, Illya G, Harmandaris V A, Müller M M, Kremer K and Deserno M 2007 Aggregation and vesiculation of membrane proteins by curvature-mediated interactions *Nature* **447** 461-464.
- [25] Ewers H, Römer W, Smith A E, Bacia K, Dmitrieff S, et. al. 2010 GM1 structure determines SV40-induced membrane invagination and infection *Nat. Cell Biol.* **12** 11-18
- [26] Römer W, Berland L, Chambon V, Gaus K, Windschiegl B, et al. 2007 Shiga toxin induces tubular membrane invaginations for its uptake into cells *Nature* **450** 670-675
- [27] Sharma P, Varma R, Sarasij R C, Ira, Gousset K, et. al. 2004 Nanoscale organization of multiple GPI-anchored proteins in living cell membranes *Cell* **116** 577-589
- [28] Goswami D, Gowrishankar K, Bilgrami S, Ghosh S, Raghupathy R, et. al. 2008 Nanoclusters of GPI-anchored proteins are formed by cortical actin-driven activity. *Cell* **135** 1085-1097
- [29] Fujita A, Cheng J, Hirakawa M, Furukawa K, Kusunoki S, et. al. 2007 Gangliosides GM1 and GM3 in the living cell membrane form clusters susceptible to cholesterol depletion and chilling *Mol. Biol. Cell* **18** 2112-2122
- [30] Plowman S J, Muncke C, Parton R G and Hancock J F 2005 H-ras, K-ras, and inner plasma membrane raft proteins operate in nanoclusters with differential dependence on the actin cytoskeleton *Proc. Natl. Acad. Sci. USA.* **102** 15500-15505
- [31] Ford M G, Mills I G, Peter B J, Vallis Y, Praefcke G J, et. al. 2002 Curvature of clathrin-coated pits driven by epsin *Nature* **419** 361-366
- [32] Henne W M, Boucrot E, Meinecke M, Evergren E, Vallis Y, et. al. 2010 FCHO proteins are nucleators of clathrin-mediated endocytosis *Science* **328** 1281-1284
- [33] van Effenterre D and Roux D 2003 Adhesion of colloids on a cell surface in competition for mobile receptors *Europhys. Lett.* **64** 543-549
- [34] Deserno M 2004 Elastic deformation of a fluid membrane upon colloid binding *Phys. Rev. E* **69** 031903
- [35] Deserno M and Bickel T 2003 Wrapping of a spherical colloid by a fluid membrane *Europhys. Lett.* **62** 767-773
- [36] Goulian M 1996 Inclusions in membranes *Curr. Opinion In Coll. & Int. Sci.* **1** 358-361
- [37] Golestanian R, Goulian M and Kardar M 1996 Fluctuation-induced interactions between rods on membranes and interfaces *Europhys. Lett.* **33** 241-245
- [38] Gov N S and Gopinathan A 2006 Dynamics of membranes driven by actin polymerization *Biophys. J.* **90** 454-469
- [39] David F 1992 *Introduction to the statistical mechanics of random surfaces and membranes* in Gross D.J., Piran T., Weinberg S. Two Dimensional Quantum Gravity and Random Surfaces, Jerusalem, Israel, Dec.27-Jan.4, 1991,, World Scientific, pp. 80-124.
- [40] Helfrich W 1973 Elastic properties of lipid bilayers: theory and possible experiments. *Z. Naturforsch. C.* **28** 693-703
- [41] Sackmann E 1995 *Biological membranes architecture and function* In Structure and Dynamics of Membranes, Vol. 1A. R. Lipowsky, and E. Sackmann, editors. Elsevier, Amsterdam, The Netherlands.
- [42] Nelson D L and Cox M M 2004 *Lehninger Principles of Biochemistry* 3rd Ed. Worth, New York
- [43] Bell G I 1978 Models for the specific adhesion of cells to cells *Science* **200** 618-627
- [44] Briggs J A G, Wilk T and Fuller S D 2003 Do lipid rafts mediate virus assembly and pseudotyping? *J. Gen. Virol.* **84** 757-768
- [45] Quinn O, Griffiths G and Warren G 1984 Density of newly synthesized plasma membrane proteins in intracellular membranes II. Biochemical studies *J. Cell Biol.* **98** 2142-2147
- [46] Lipowsky R and Döbereiner H G 1998 Vesicles in contact with nanoparticles and colloids *Europhys. Lett.* **43** 219-225
- [47] Yuan H, Li J, Bao G and Zhang S 2010 Variable nanoparticle-Cell adhesion strength regulates cellular uptake *Phys. Rev. Lett.* **105** 138101
- [48] Yuan H, Huang C and Zhang S 2010 Virus-inspired design principles of nanoparticle-based bioagents *PLoS ONE* **5** e13495
- [49] Müller M M, Deserno M and Guven J 2005 Interface-mediated interactions between particles: A geometrical

approach *Phys. Rev. E* **72** 061407  
[50] Müller M M, Deserno M and Guven J 2005 Geometry of

surface-mediated interactions *Europhys. Lett.* **69** 482-488